Numerical Simulation of Contaminant Distribution Around a Modeled Human Body: CFD Study on Computational Thermal Manikin—Part II

Shuzo Murakami, Dr.Eng. Member ASHRAE
Shinsuke Kato, Dr.Eng. Member ASHRAE
Jie Zeng

ABSTRACT

The rising stream around a human body attributable to metabolic heat can carry contaminants from the floor level to the human breathing system. Thus, the quality of the breathing air greatly depends on the concentration distribution in the lower part of the room and the characteristics of the local air motion around the body. In this paper, a modeled human body (computational thermal manikin) is placed in a room that is air-conditioned with a displacement ventilation system. Flow and temperature fields around the manikin are analyzed by computational fluid dynamics (CFD) using a low-Reynolds-number type k-ε model. Based on the predicted flow field, the age of supply air and the residual lifetime of air in the room are also numerically calculated by CFD. Three cases of prediction of the concentration distribution are carried out with different locations of contaminant generation. The quality of the breathing air is assessed using the newly defined index, indicating the effective entrainment ratio of the lower region air to the breathing air. Results of the CFD analysis agree well with previous experimental data.

INTRODUCTION

In a previous paper (Murakami et al. 1997), the local air motions around a modeled human body (computational thermal manikin) that is placed in various types of flow field were analyzed by computational fluid dynamics (CFD). The rising stream observed around the manikin plays an important role in the characteristics of convective heat transfer from the manikin. It also carries contaminants from the floor level to the human breathing zone. The phenomenon has been examined experimentally (Kim et al. 1991; Brohus and Nielsen 1994; Hyldgaard 1994). This paper focuses on the effect of the rising stream on the quality of the breathing air and evaluates it with the aid of CFD analysis. However, the effect of breathing is not taken into account at this stage.

The displacement ventilation system is widely used because of its high ventilation efficiency. This system can supply relatively fresh and cooled air directly to an occupied zone. One of the important characteristics of this system is the ability to produce vertical temperature stratification. Such stratification suppresses the vertical mixing of air so that a vertical concentration gradient appears (Hyldgaard 1994). This enables the occupied zone to be kept clean and thermally comfortable. In this type of stagnant flow field, the rising stream generated around a human body by metabolic heat becomes the essential factor in transporting air from lower to higher levels (Kim et al. 1991). Under these circumstances, the contaminant concentration distribution depends on two decisive factors: (a) the position of the contaminant generation and (b) the vertical transport properties from the rising stream.

In this paper, utilizing ventilation efficiency indices, the relationship between the concentration distribution and the above decisive factors is analyzed. The indices used here are (a) the age of supply air, (b) the residual lifetime of air (Murakami 1992; Kato et al. 1992), and (c) the effective entrainment ratio of the lower air to the breathing air. This ratio was first proposed as the effectiveness of entrainment in the human boundary layer by Brohus and Nielsen (1994), then modified by the authors (Kato et al. 1996).

EFFECTIVE ENTRAINMENT RATIO OF THE LOWER AIR TO THE BREATHING AIR

In a room with a displacement ventilation system, there is usually an apparent vertical stratification of concentration distribution. Using the characteristics of this stratification, the room space is divided into several zones. As shown in Figure 1, inasmuch as the steep concentration gradient in the vertical direction appears at the middle height of the space, it is possible to divide the room space into two zones, the lower and the upper zone. The third zone is defined around the human body.

Shuzo Murakami is a professor, **Shinsuke Kato** is an associate professor, and **Jie Zeng** is a post-graduate student at the Institute of Industrial Science (IIS), University of Tokyo, Japan.

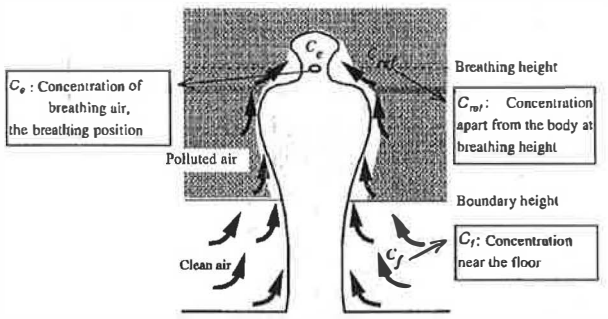

Figure 1 *Entrainment of lower air to breathing air ($\eta^*_e > 0$).*

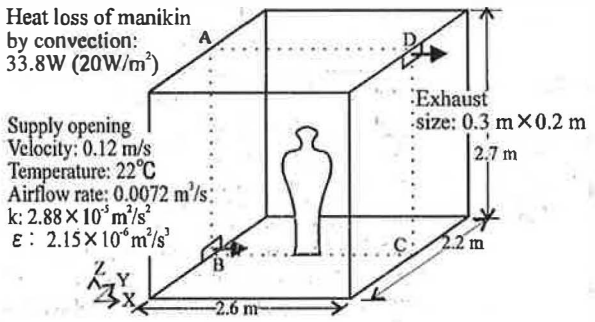

Figure 2 *Flow field analyzed.*

This zone is characterized by the rising stream attributable to metabolic heat production.

To evaluate the effect of entrainment and transport of air from the lower zone to the breathing position, Brohus and Nielsen (1994) proposed the concept of the effective entrainment ratio of the lower air to the breathing air, which is expressed in Equation 1.

$$\eta_e = (C_{ref} - C_e)/(C_{ref} - C_f) \quad (1)$$

where

C_e = contaminant concentration of breathing air (cf. Figure 1),

C_{ref} = contaminant concentration apart from the body at breathing height,

C_f = contaminant concentration near the floor.

$$C_e = \eta_e C_f + (1 - \eta_e) C_{ref} \quad (2)$$

As shown in Equation 2, the breathing air is composed of the air in the lower zone of the room (C_f) and the air apart from the body at breathing height (C_{ref}). η_e shows the mixing ratio of these two components. Thus, η_e means the ability to entrain the air in the lower zone and to transport it to the breathing position by the rising stream. Considering the quality of breathing air, the authors extended η_e to η^*_e (the modified effective entrainment ratio of the lower air to the breathing air), which is shown in Equation 3 (Figure 1, Note A).

$$\eta^*_e = \eta_e \cdot sig(C_{ref} - C_f) = (C_{ref} - C_e)/|C_{ref} - C_f| \quad (3)$$

Here, $C_f \le C_e \le C_{ref}$ or $C_{ref} \le C_e \le C_f$ is assumed.

$sig(x)$ = sign function, $x \ge 0$ $sig = 1$, $x < 0$ $sig = -1$

Depending on whether the air in the lower zone is clean or not, η^*_e has plus or minus value. If the air in the lower zone is relatively clean, and this clean air is transported to the breathing position by the rising stream, η^*_e becomes larger than 0. This shows the positive effect of the entrainment. If the air in the lower region is relatively dirty, η^*_e becomes less than 0, showing the negative effect of the entrainment on the quality of the breathing air. In the case of $\eta^*_e = 1$, the air in the lower zone is clean, and the breathing air is completely transported from there. The breathing air is not mixed with the air at the breathing height. In the case of $\eta^*_e = -1$, the breathing air is completely composed of the dirty air from the lower zone. In the case of $C_e = C_{ref}$, $\eta^*_e = 0$, the breathing air comes from the breathing height, and the rising stream around the body has no influence on the quality of the breathing air (Note B).

With CFD simulation, the concentration of contaminants in the room is easily calculated and the representative concentration of each divided zone is easily estimated. In this paper, the representative concentration of each zone, such as C_{ref}, C_f, refers to the mean value of contaminant concentration through each zone.

CFD METHODS

The flow field analyzed is shown in Figure 2. A heated manikin is placed in a room that is air conditioned with a displacement ventilation system. The shape of the manikin is simplified from a real human body shape, with feet and arms put together close to the body. The manikin has the standard height (1.651 m) and weight (65.5 kg) of a Japanese male adult. The area of manikin skin surface is calculated as 1.688 m^2 (SHASE 1987). The metabolic heat production for a standing, relaxed human body is recommended as 70 W/m^2 (1.2 met) (ASHRAE 1993). It is reasonable to assume that heat loss from the body by convection is about one-third of the total metabolic heat production in the normal indoor environment. This paper is only concerned with convective heat transfer. Thus, the manikin is simply specified to uniformly release heat by convection at 20 W/m^2 through the whole surface. This becomes the boundary condition of the manikin surface for solving the temperature transport equation. In order to remove convective heat loss from the manikin and to ensure the exhaust temperature at 27°C, the supply temperature is specified at 22°C for the low supply velocity at 0.1 2 m/s. The airflow rate, air change rate, and nominal time constant of the room are about 25.9 m^3/h, 1.7 ACH, and 0.6 h, respectively. The air change rate is slightly lower than that of a normal displacement ventilation system (about 5 ACH). The CFD analysis is conducted based on a Launder-Sharma type, low-Reynolds-number, k-ε turbulence model (Launder and Sharma 1974). Tables 1 and 2 detail the numerical methods

BACK TO PAGE ONE

TABLE 1
Numerical Methods

Turbulence Model	Low-Reynolds-number k-ε model (Launder-Sharma Type)
Numerical Schemes	Space difference: hybrid Time difference: backward
Grid system	Computational domain is discretized into 125,568 cells with BFC. In the normal direction of the manikin surface, the grid is spaced with geometric progression. The y^+ of the first cell near the manikin is less than 5. Considering the symmetrical property of the flow field, half of the space is calculated.

TABLE 2
Boundary Conditions

Supply Opening	$U_{in} = 0.12$ m/s, $T_{in} = 22°C$, $k_{in} = 0.002\ U_{in}^2$, $\varepsilon_{in} = k_{in}^{3/2}/(0.3D)$; $D = 0.24$ m
Exhaust Opening	U, k, ε, T: free slip
Wall Boundary	$U, k, \tilde{\varepsilon}: U_w = 0,\ k_w = (\partial k/\partial x_i)_w = 0,\ (\tilde{\varepsilon})_w = 0$
	adiabatic wall: $(\partial T/\partial x_i)_w = 0$ Manikin surface: $Q_w = 20$ W/m^2 (quantity of convective heat loss)

and boundary conditions. The contaminants are considered as passive scalar particles. This means the contaminants have the same properties, such as density, viscosity, velocity, etc., as those of air. The CFD method is detailed in a previous paper (Murakami et al. 1997).

CHARACTERISTICS OF FLOW AND TEMPERATURE FIELDS

The flow field is shown in Figure 3. It is clear that the warm rising stream appears around the manikin, while the flow field apart from the body is almost stagnant. In the upper zone above the manikin, a rising thermal plume is obvious. It reaches a maximum velocity of 0.26 m/s.

The temperature field is shown in Figure 4. A vertical temperature gradient appears in the room with the displacement ventilation system. Between the feet and the waist level of the body (Figure 4), the gradient becomes very steep. However, the vertical temperature gradient is slightly steeper than in the case of considering the radiation as well as the convection, which corresponds better to the actual situation (Zeng et al. 1997). As a result, the effect of the rising stream is slightly overpredicted. The mean air temperature of the room is calculated as 26.0°C, and the mean temperature of the manikin surface is 31.0°C (Murakami et al. 1997). There is about 5.0°C temperature difference between the manikin surface and the surrounding air. This corresponds to an actual situation in a normal indoor environment.

As stated above, the room space is divided into three zones: the upper zone, the lower zone, and the zone around the

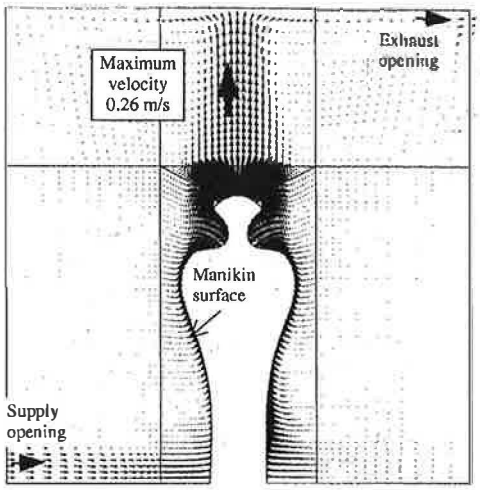

Figure 3 *Velocity distribution.*

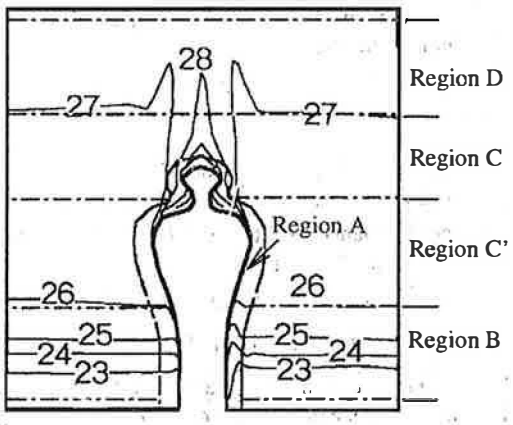

Figure 4 *Temperature distribution (Section ABCD: °C)*

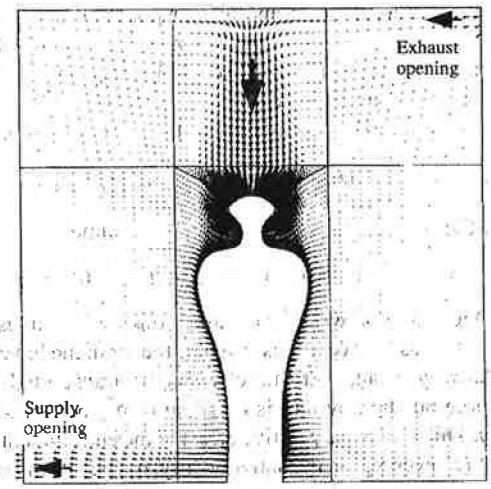

Figure 5 *Virtual velocity field with time reversed.*

TABLE 3
Cases of Contaminant Diffusion Simulation

	Position of Contaminant Source	Flow Field
Case 1	Uniform generation throughout room	Shown in Figure 3
Case 2	As above	Virtual flow field with time-reversed
Case 3	Uniform generation from ceiling	Shown in Figure 3
Case 4	Uniform generation from floor	As above
Case 5	Uniform generation from manikin surface	As above

body. In this paper, the authors call the lower zone Region B. The upper zone is divided into three regions: Regions C', C, and D (Figure 4 and Note A). The mean concentration of Region B is defined as C_f and that of Region C as C_{ref}.

Figure 5 shows a time-reversed virtual flow field obtained from the real flow field shown in Figure 3. As the reversed time passes, the flow comes from the exhaust opening, diverges into the room space, converges, and returns to the supply opening. By using the virtual flow field, the residual lifetime of air is easily calculated with uniform contaminant generation throughout the space (Kato et al. 1992).

CALCULATION OF CONCENTRATION DISTRIBUTION

Cases Analyzed

Five cases are analyzed here. Table 3 shows the details of each case. The age of the supply air is the average time taken for supply air (fresh) entering the space to reach any specified location within the space. In Case 1, the contaminants are generated uniformly throughout the room; thus, the predicted contaminant concentration corresponds to the age of the supply air (Kato et al. 1992). The distribution of the age of supply air can explain how effective ventilation is in getting fresh air to the body. The residual lifetime of air is the time taken for air at any location to be exhausted from the space. In Case 2, the position of contaminant generation is the same as in Case 1. The time-reversed virtual flow field (Figure 5), however, is used here. The predicted contaminant concentration indicates the residual lifetime of air. From this case, the ventilation efficiency in removing contaminants from the vicinity of the manikin is analyzed. In Case 3, the contaminants are generated uniformly from the ceiling. This corresponds to an actual situation in which the contaminants, such as volatile organic compounds, are generated from the paint of the ceiling surface. In this case, the air in the lower zone of the room is relatively clean. In Case 4, contrary to Case 3, the contaminants are generated uniformly from the floor. The contaminants, including dust generated from the floor, have a large influence on the indoor air quality. In Case 5, the contaminants are generated uniformly from the manikin surface. In this case, the bioeffluent of the human body is examined. In all cases, the contaminant concentration is nondimensionalized by the perfect mixing concentration (which equals the average contaminant concentration of the exhaust opening).

Case 1: Uniform Generation of Contaminants Throughout the Room (Age of Supply Air)

The concentration distribution in Case 1 is shown in Figure 6a and Table 4. This corresponds to the age of supply air. The mean age of supply air in Region B is 0.30. Compared with the other regions, this is the minimum value because the fresh air is supplied directly to Region B from the supply opening located near the floor. The breathing air has a value of 0.50, lower than that of the air at the breathing height (1.28). The young air is entrained and transported to the breathing position from the lower part of the room (Region B) by the rising stream. Some part of the rising stream around the manikin is exhausted through the exhaust opening near the ceiling. The rest descends to the lower region apart from the body and then becomes old. In Region D, it has a value of 1.1. The age of air becomes more than 1.8 in the region between the body's waist and breast levels. This is the highest value in the room. The obvious boundary line between the highest and the lowest value region is observed at waist level. In Case 1 the modified effective entrainment ratio of the lower air to the breathing air is 79% (Table 4). This means 79% of the breathing air can be provided from Region B, where air is relatively young and fresh, by the rising stream.

Case 2: Uniform Generation of Contaminants Throughout the Room with Time-Reversed Virtual Field (Residual Lifetime of Air)

The concentration distribution in Case 2 is shown in Figure 6b and Table 4. This corresponds to the residual lifetime of air. The air near the exhaust opening has the lowest value and is quickly exhausted. The air in Region B has the maximum value of 0.96 and takes much longer to be exhausted. Concerning the two sides of the human body, the right-hand region near the exhaust opening has lower values than that of the left. This means that the air in the right-hand region takes less time to be exhausted. The mean residual lifetime of the whole space is 0.91. The breathing air, however, has a lower value of 0.50. The value in Region A also becomes low at 0.69. These low values mean that the air is driven by the rising stream around the body, rises to the upper space, and is then quickly exhausted. Thus, the contaminants can be quickly removed from the vicinity of the body by the rising stream.

Case 3: Uniform Generation of Contaminants from the Ceiling

The concentration distribution in Case 3 is shown in Figures 6c and 7 and Table 4. The concentration stratification at the waist level of the manikin is clearly observed. This steep, vertical concentration gradient corresponds to the obvious boundary between the highest and lowest concentration

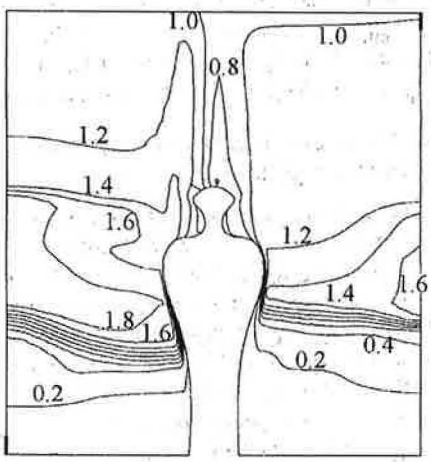

(a) Case 1—Age of supply air (Contaminant source: uniform in the space).

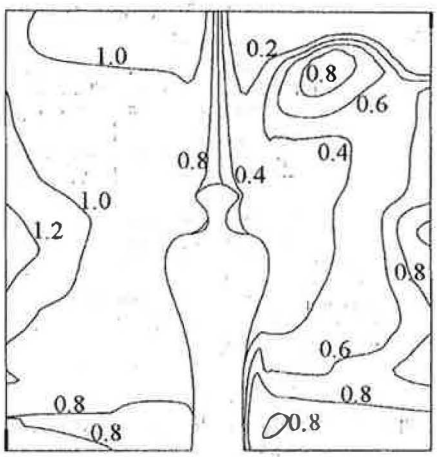

(b) Case 2—Residual lifetime of air (Contaminant source: uniform in the space; flow field: time-reversed).

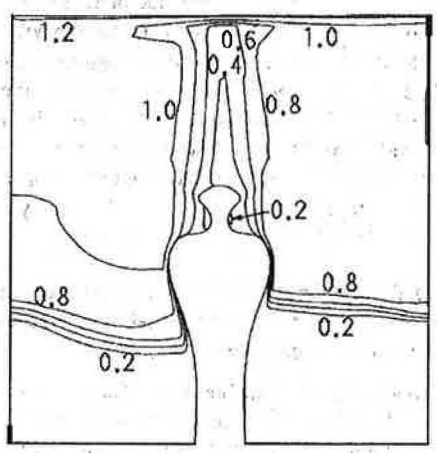

(c) Case 3 (Contaminant source: ceiling surface).

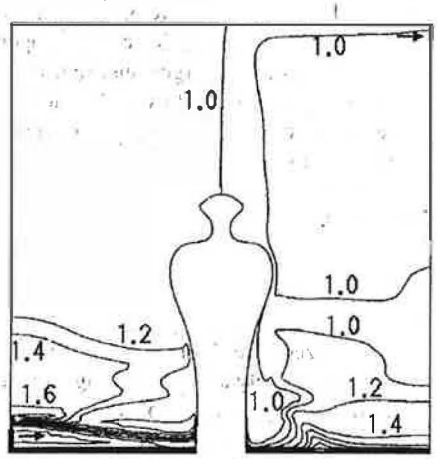

(d) Case 4 (Contaminant source: floor surface).

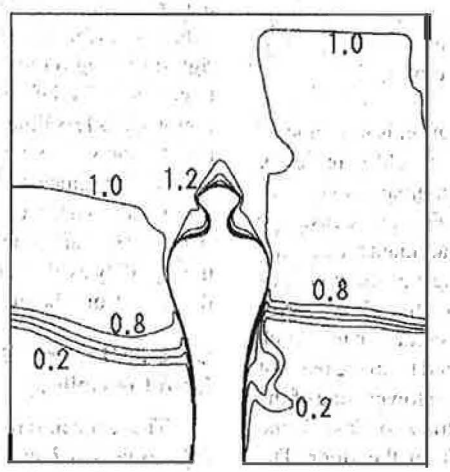

(e) Case 5 (Contaminant source: manikin surface).

Figure 6 *Concentration distribution (Section ABCD).*

BACK TO PAGE ONE

TABLE 4
C_f, C_{ref}, C_e, and η_e^*

		Case 1	Case 2	Case 3	Case 4	Case 5
Concentration	Mean Concentration of Room	0.91	0.91	0.60	1.05	0.63
	Region A (near the manikin)	0.68	0.69	0.37	0.99	0.54
	Region B (the lower zone: C_f)	0.30	0.96	0.02	1.20	0.06
	Region C'	0.91	0.95	0.43	1.06	0.46
	Region C (breathing height: C_{ref})	1.28	0.95	0.94	1.04	0.98
	Region D	1.10	0.80	1.00	1.04	1.00
	Breathing Air: C_e	0.50	0.50	0.25	1.15	1.20
Modified Effective Entrainment Ratio of Lower Air to Breathing Air η_e^*		79%	—	75%	−69%	—

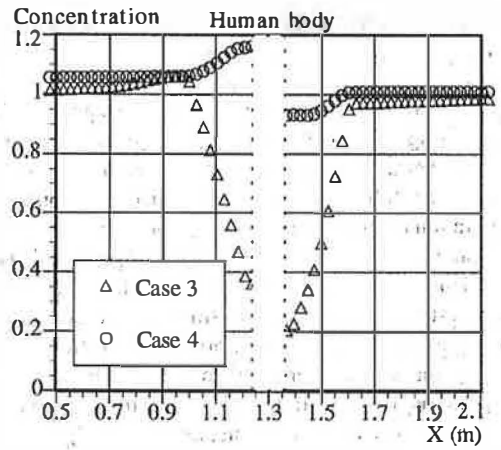

Figure 7 Horizontal concentration distribution at breathing level (Z = 1.45 m).

regions observed in Case 1. The mean contaminant concentration throughout the room is 0.60. The value in Region B is relatively low at 0.02, but in Region D it becomes higher at 1.00, equaling the contaminant concentration of the exhaust opening. The contaminant concentration of the breathing air becomes much lower (0.25) than that of Region C (0.94), which is located at the breathing height. This is caused by the entrainment effect of the clean air in Region B attributable to the rising stream. The characteristics are also observed in Figure 7. The modified effective entrainment ratio of the lower air to the breathing air is 75%, corresponding well with Case 1. The value of 75% means that 75% of the breathing air is transported from Region B where the air is relatively clean. The quality of the breathing air in Case 3 is quite good, although the contaminant concentration at the breathing height is rather high. The phenomena are also confirmed by the experiment (Brohus and Nielsen 1994).

Case 4: Uniform Generation of Contaminants from the Floor

The concentration distribution in Case 4 is shown in Figures 6d and 7 and Table 4. Inasmuch as the contaminants are generated from the floor, the contaminants tend to stay in the lower region (Region B), where the mean contaminant concentration is high at 1.20. In Case 4, the contaminant concentration is distributed almost uniformly in the other regions of the room (Regions C, C', and D: 1.04 - 1.06). This distribution property is different from the other cases in which the concentration stratification is clearly observed. The contaminant concentration of the breathing air (1.15) is higher than that of Region C (1.04) because the dirty air in Region B (1.04) converges around the body and then rises to the breathing position (Figure 7). The modified effective entrainment ratio of the lower air to the breathing air is −69%. The absolute value corresponds well with Cases 1 and 3. The characteristics show that to improve the quality of the breathing air in a room with a displacement ventilation system, it is important to avoid contaminant generation in the lower part of the room.

Case 5: Uniform Generation of Contaminants from the Manikin Surface

The concentration distribution in Case 5 is shown in Figure 6e and Table 4. The contaminants generated from the manikin surface are transported from the lower to the upper region with the rising stream. The maximum vertical gradient of contaminant concentration appears at waist level, where the concentration stratification is clearly observed. The mean contaminant concentration throughout the room is 0.63. Below the steep vertical concentration gradient, the mean contaminant concentration in Region B is relatively low at 0.06. Conversely, the contaminant concentration of the upper region above the body head is high at 1.00, which equals that of the exhaust opening. The concentration of the breathing air is higher at 1.20 because the contaminants are generated from the body surface itself. In this case (one person in a room), the concept of the effective entrainment ratio of the lower air to the breathing air is not available (Note B). However, in the situa-

BACK TO PAGE ONE

tion where many people are in a room, the contaminant concentration in the upper zone of the room is proportional to the number of people and becomes higher. The breathing air, however, is still relatively clean because the people do not contaminate the air in the lower zone.

CONCLUSIONS

1. Similar to temperature stratification, concentration stratification also appears in the stagnant flow field in a room that is air-conditioned with a displacement ventilation system. This property is clearly explained by the distribution of the age of supply air.
2. The rising stream from metabolic heat production, as well as the concentration stratification, has great influence on the quality of the breathing air. These characteristics are clearly comprehensible with the distribution of the age of supply air and the residual lifetime of air.
3. To evaluate the influence of the entrainment effect with the rising stream on the quality of the breathing air, the modified effective entrainment ratio of the lower air to the breathing air is proposed. The usefulness of the index is demonstrated with several locations of contaminant generation.
4. If the rising stream around the body surface is not broken by the surrounding airflow, whether it enhances or decreases the quality of the breathing air depends on the location of the contaminant generation. The rising stream has a positive influence on the quality of the breathing air when the contaminants are generated in the upper part of the room, above the breathing height, and the air in the lower part of the room is relatively clean. Conversely, the rising stream has a negative effect when the contaminant is generated in the lower part of the room, below the breathing height, and the air in the lower part is relatively dirty.

NOMENCLATURE

A = area of supply opening, m^2
C_e = contaminant concentration of breathing air
C_f = contaminant concentration near floor
C_{ref} = contaminant concentration apart from body at breathing height
D = hydraulic diameter, $D = 4A/P$, m
k = turbulent energy, m^2/s^2
P = perimeter of supply opening, m
Q = convective heat transfer rate, W/m^2
T = mean temperature, °C
U = mean velocity, m/s
ε = dissipation rate of turbulent energy, m^2/s^3, $\tilde{\varepsilon} = \varepsilon - \nu(\partial k^{1/2}/\partial x)^2$
η_e = effective entrainment ratio of lower air to breathing air
η^*_e = modified effective entrainment ratio of lower air to breathing air

Subscripts

i = 1, 2, and 3, denotes x, y, and z directions, respectively
in = value of supply opening
w = value of surface

NOTE A

In this paper, to estimate the representative concentrations such as C_f and C_{ref}, the author divided the room space into five regions: Region A, around the manikin within 30 cm, where the rising stream is located; Region B, between floor level and waist level, where the temperature gradient is steepest; Region C', up to the neck level; Region C, up to a little higher than head level, called the breathing height; and Region D, the remainder.

NOTE B

There are actually a few cases in which the boundary between the zones of high concentration and low concentration cannot be clearly differentiated. The applicability of differentiating these two zones in the given space would require further discussion. The index η^*_e cannot be well estimated in the following cases: (a) when the contaminant concentration is distributed almost uniformly and the concentration stratification does not obviously appear, which often occurred in the room with a traditional mixing-type air-conditioning system; (b) when the position of the concentration stratification is located above the breathing position; (c) when the contaminants are generated from a human body's surface, the contaminant concentration of the breathing air cannot be decided by those two components, i.e., C_f and C_{ref}.

REFERENCES

ASHRAE. 1993. *1993 ASHRAE handbook—Fundamentals*, Chapter 8. Atlanta: American Society of Heating, Refrigerating and Air-Conditioning Engineers, Inc.

Brohus, H., and P.V. Nielsen. 1994. Contaminant distribution around persons in rooms ventilated by displacement ventilation. *Proceedings of Roomvent '94, Poland,* pp. 294-312.

Hyldgaard, C.E. 1994. Humans as a source of heat and air pollution. *Proceedings of Roomvent '94, Poland,* pp. 413-433.

Kato, S., S. Murakami, and H. Kobayashi. 1992. New scales for evaluating ventilation efficiency as affected by supply and exhaust openings based on spatial distribution of contaminants. *Proceedings of ISRACVE, University of Tokyo*, pp. 321-332.

Kato, S., S. Murakami, and J. Zeng. 1996. Numerical analysis of contaminant distribution around a human body. *ROOMVENT '96,* Vol. 2, pp. 129-136.

Kim, I.G., H. Homma, and E. Ninomiya. 1991. Movement and distribution of occupant product ventilation subjects in a room. Part 8, Influence of numbers of models on

BACK TO PAGE ONE

ventilation efficiency. *Proceedings of Annual Technical Meeting of SHASE*, pp. 1093-1096 (in Japanese).

Launder, B.E., and B.I. Sharma. 1974. Application of the energy-dissipation model of turbulence to the calculation of flow near a spinning disc. *Letters in Heat and Mass Transfer* 1: 131-138.

Murakami, S. 1992. New scales for ventilation efficiency and their application based on numerical simulation of room airflow. *Proceedings of ISRACVE, University of Tokyo,* pp. 22-37.

Murakami, S., S. Kato, and J. Zeng. 1997. Flow and temperature fields around human body with various room air distributions, CFD study on computational thermal manikin—Part 1. *ASHRAE Transactions* 103 (1): 3-15.

SHASE. 1987. Benran 1 (fundamentals), Chapter 3 (in Japanese).

Zeng, J., S. Murakami, S. Kato, and T. Hayashi. 1997. Study on computational thermal manikin—Part 9, Coupled simulation of convective and radiant heat transfer of thermal manikin with low-Reynolds-number type k-ε (B model). *Proceedings of Annual Technical Meeting of SHASE*, pp. 101-104 (in Japanese).